

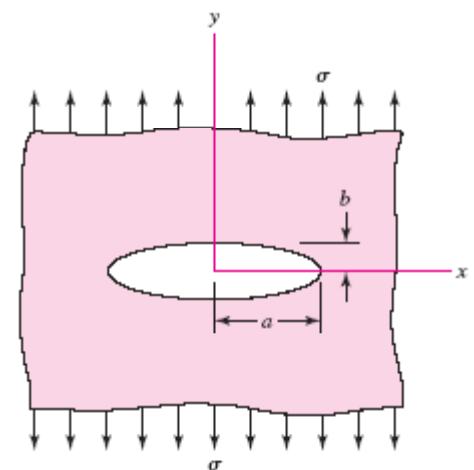
# Introduction to Fracture mechanics

# Introduction to Fracture Mechanics

The idea that cracks exist in parts even before service begins, and that cracks can grow during service, has led to the descriptive phrase “damage-tolerant design.” The focus of this philosophy is on crack growth until it becomes critical, and the part is removed from service. The analysis tool is *linear elastic fracture mechanics* (LEFM). Inspection and maintenance are essential in the decision to retire parts before cracks reach catastrophic size. Where human safety is concerned, periodic inspections for cracks are mandated by codes and government ordinance.

The foundation of fracture mechanics was first established by Griffith in 1921 using the stress field calculations for an elliptical flaw in a plate developed by Inglis in 1913. For the infinite plate loaded by an applied uniaxial stress  $\sigma$  in Fig. 5–22, the maximum stress occurs at  $(\pm a, 0)$  and is given by

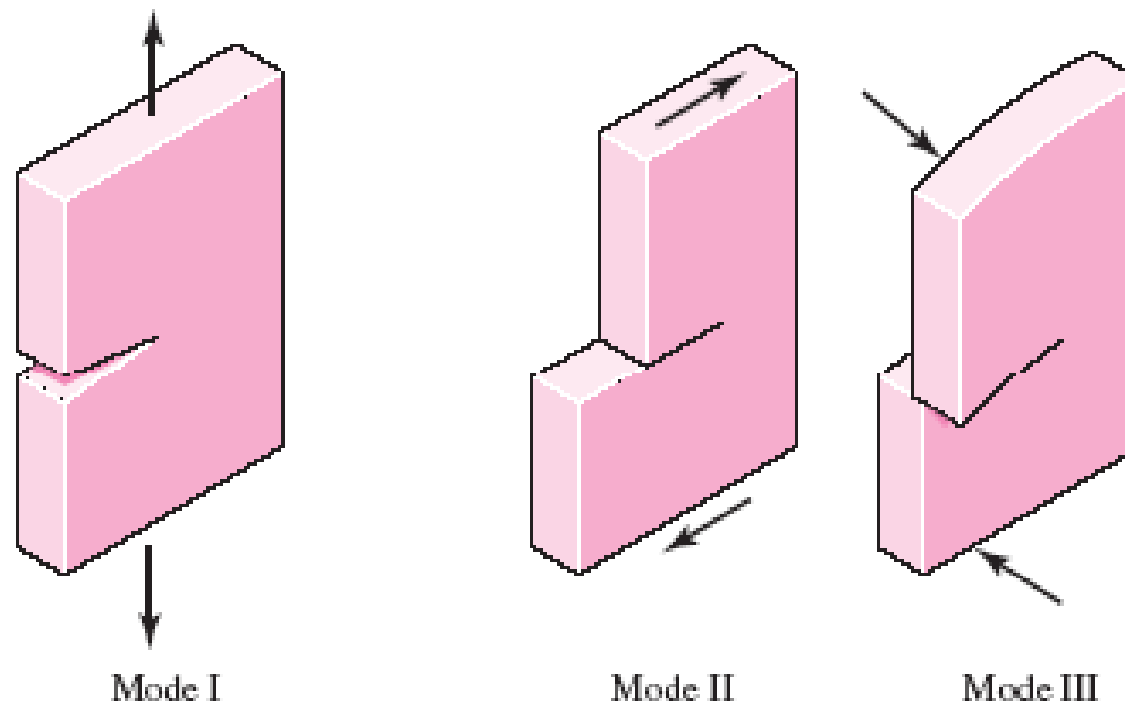
$$(\sigma_y)_{\max} = \left(1 + 2\frac{a}{b}\right)\sigma$$



Note that when  $a = b$ , the ellipse becomes a circle and Eq. (5-33) gives a stress concentration factor of 3. This agrees with the well-known result for an infinite plate with a circular hole (see Table A-15-1). For a fine crack,  $b/a \rightarrow 0$ , and Eq. (5-34) predicts that  $(\sigma_y)_{\max} \rightarrow \infty$ . However, on a microscopic level, an infinitely sharp crack is a hypothetical abstraction that is physically impossible, and when plastic deformation occurs, the stress will be finite at the crack tip.

## Crack Modes and the Stress Intensity Factor

Three distinct modes of crack propagation exist, as shown in Fig. 5–23. A tensile stress field gives rise to mode I, the *opening crack propagation mode*, as shown in Fig. 5–23a. This mode is the most common in practice. Mode II is the *sliding mode*, is due to in-plane shear, and can be seen in Fig. 5–23b. Mode III is the *tearing mode*, which arises from out-of-plane shear, as shown in Fig. 5–23c. Combinations of these modes can also occur. Since mode I is the most common and important mode, the remainder of this section will consider only this mode.



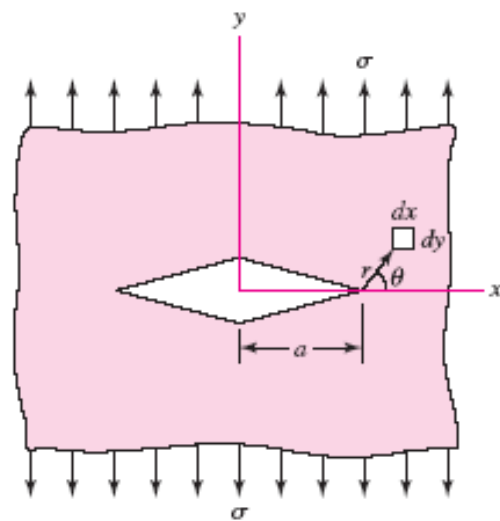
Consider a mode I crack of length  $2a$  in the infinite plate of Fig. 5-24. By using complex stress functions, it has been shown that the stress field on a  $dx\,dy$  element in the vicinity of the crack tip is given by

$$\sigma_x = \sigma \sqrt{\frac{a}{2r}} \cos \frac{\theta}{2} \left( 1 - \sin \frac{\theta}{2} \sin \frac{3\theta}{2} \right) \quad (5-34a)$$

$$\sigma_y = \sigma \sqrt{\frac{a}{2r}} \cos \frac{\theta}{2} \left( 1 + \sin \frac{\theta}{2} \sin \frac{3\theta}{2} \right) \quad (5-34b)$$

$$\tau_{xy} = \sigma \sqrt{\frac{a}{2r}} \sin \frac{\theta}{2} \cos \frac{\theta}{2} \cos \frac{3\theta}{2} \quad (5-34c)$$

$$\sigma_z = \begin{cases} 0 & \text{(for plane stress)} \\ \nu(\sigma_x + \sigma_y) & \text{(for plane strain)} \end{cases} \quad (5-34d)$$



define a factor  $K$  called the *stress intensity factor* given by

$$K = \sigma \sqrt{\pi a} \quad (b)$$

where the units are  $\text{MPa}\sqrt{\text{m}}$  or  $\text{kpsi}\sqrt{\text{in.}}$ . Since we are dealing with a mode I crack, Eq. (b) is written as

$$K_I = \sigma \sqrt{\pi a} \quad (5-35)$$

The stress intensity factor is *not* to be confused with the static stress concentration factors  $K_t$  and  $K_{ts}$  defined in Secs. 3-13 and 5-2.

Thus Eqs. (5-34) can be rewritten as

$$\sigma_x = \frac{K_I}{\sqrt{2\pi r}} \cos \frac{\theta}{2} \left( 1 - \sin \frac{\theta}{2} \sin \frac{3\theta}{2} \right) \quad (5-36a)$$

$$\sigma_y = \frac{K_I}{\sqrt{2\pi r}} \cos \frac{\theta}{2} \left( 1 + \sin \frac{\theta}{2} \sin \frac{3\theta}{2} \right) \quad (5-36b)$$

$$\tau_{xy} = \frac{K_I}{\sqrt{2\pi r}} \sin \frac{\theta}{2} \cos \frac{\theta}{2} \cos \frac{3\theta}{2} \quad (5-36c)$$

$$\sigma_z = \begin{cases} 0 & \text{(for plane stress)} \\ \nu(\sigma_x + \sigma_y) & \text{(for plane strain)} \end{cases} \quad (5-36d)$$

The stress intensity factor is a function of geometry, size and shape of the crack, and the type of loading. For various load and geometric configurations, Eq. (5-35) can be written as

$$K_I = \beta \sigma \sqrt{\pi a} \quad (5-37)$$

where  $\beta$  is the *stress intensity modification factor*. Tables for  $\beta$  are available in the literature for basic configurations.<sup>11</sup> Figures 5-25 to 5-30 present a few examples of  $\beta$  for mode I crack propagation.

## Fracture Toughness

When the magnitude of the mode I stress intensity factor reaches a critical value,  $K_{Ic}$  crack propagation initiates. The *critical stress intensity factor*  $K_{Ic}$  is a material property that depends on the material, crack mode, processing of the material, temperature, loading rate, and the state of stress at the crack site (such as plane stress versus plane strain). The critical stress intensity factor  $K_{Ic}$  is also called the *fracture toughness* of the material. The fracture toughness for plane strain is normally lower than that for plane stress. For this reason, the term  $K_{Ic}$  is typically defined as the *mode I, plane strain fracture toughness*. Fracture toughness  $K_{Ic}$  for engineering metals lies in the range  $20 \leq K_{Ic} \leq 200 \text{ MPa} \cdot \sqrt{\text{m}}$ ; for engineering polymers and ceramics,  $1 \leq K_{Ic} \leq 5 \text{ MPa} \cdot \sqrt{\text{m}}$ . For a 4340 steel, where the yield strength due to heat treatment ranges from 800 to 1600 MPa,  $K_{Ic}$  decreases from 190 to 40  $\text{MPa} \cdot \sqrt{\text{m}}$ .

**Table 5-1**

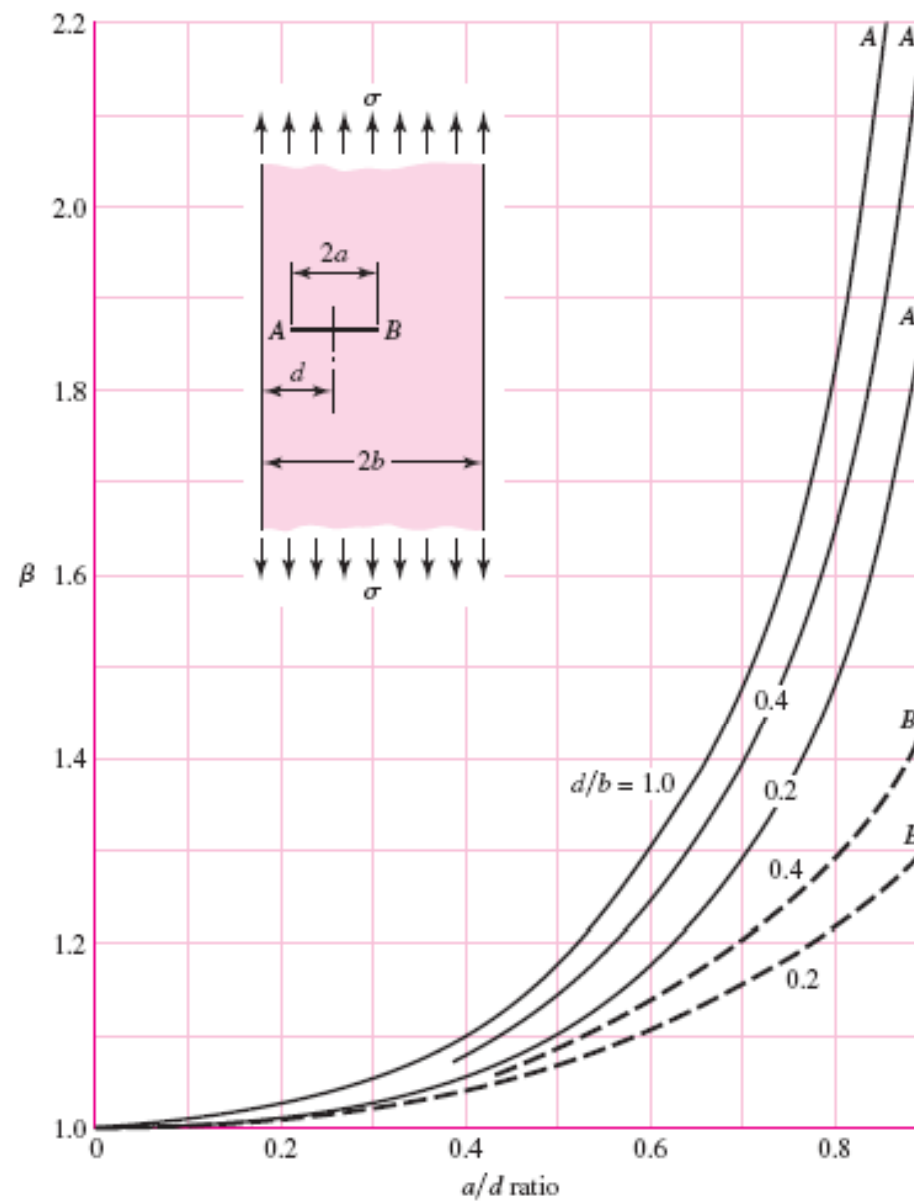
Values of  $K_{Ic}$  for Some  
Engineering Materials  
at Room Temperature

Material	$K_{Ic}$ , MPa $\sqrt{m}$	$S_y$ , MPa
Aluminum		
2024	26	455
7075	24	495
7178	33	490
Titanium		
Ti-6Al-4V	115	910
Ti-6Al-4V	55	1035
Steel		
4340	99	860
4340	60	1515
52100	14	2070



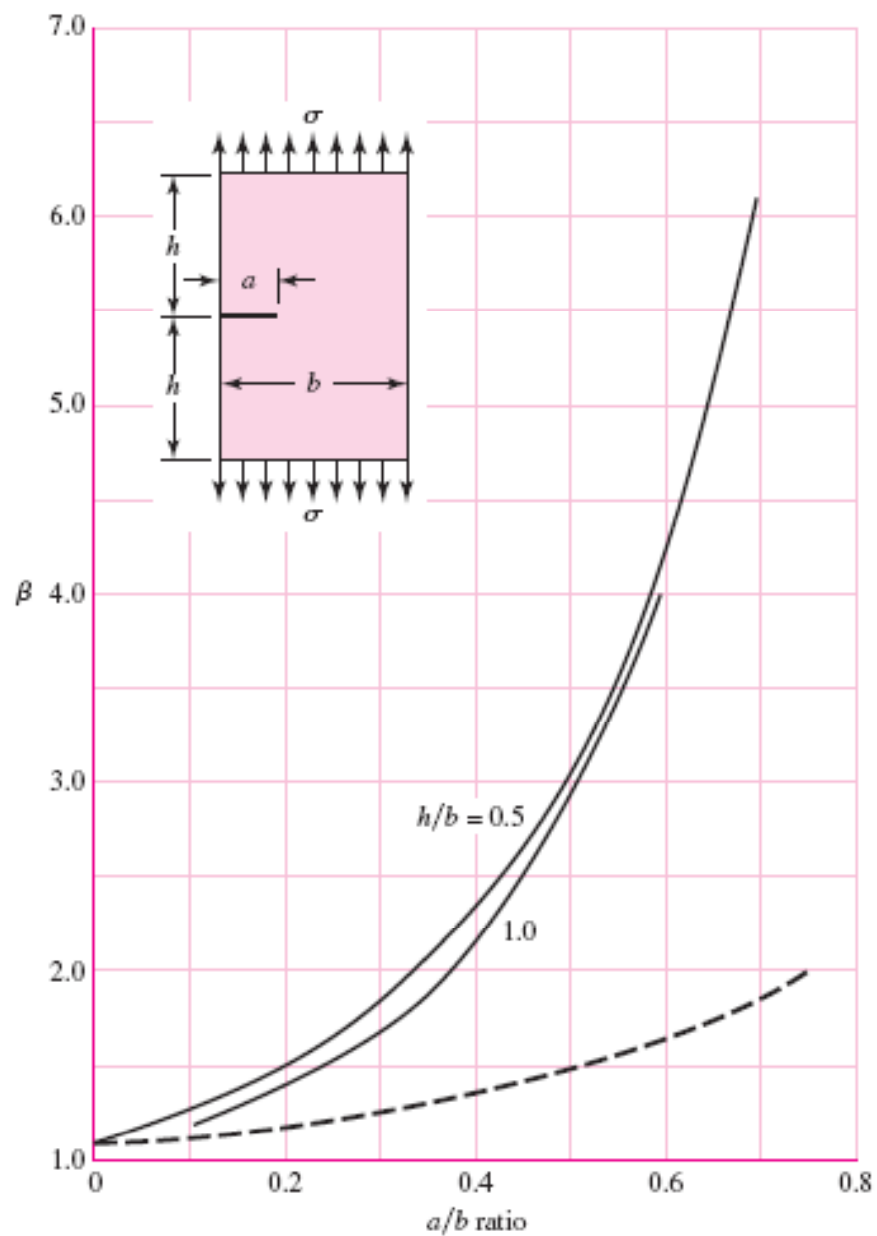
**Figure 5-25**

Offcenter crack in a plate in longitudinal tension; solid curves are for the crack tip at A; dashed curves are for the tip at B.



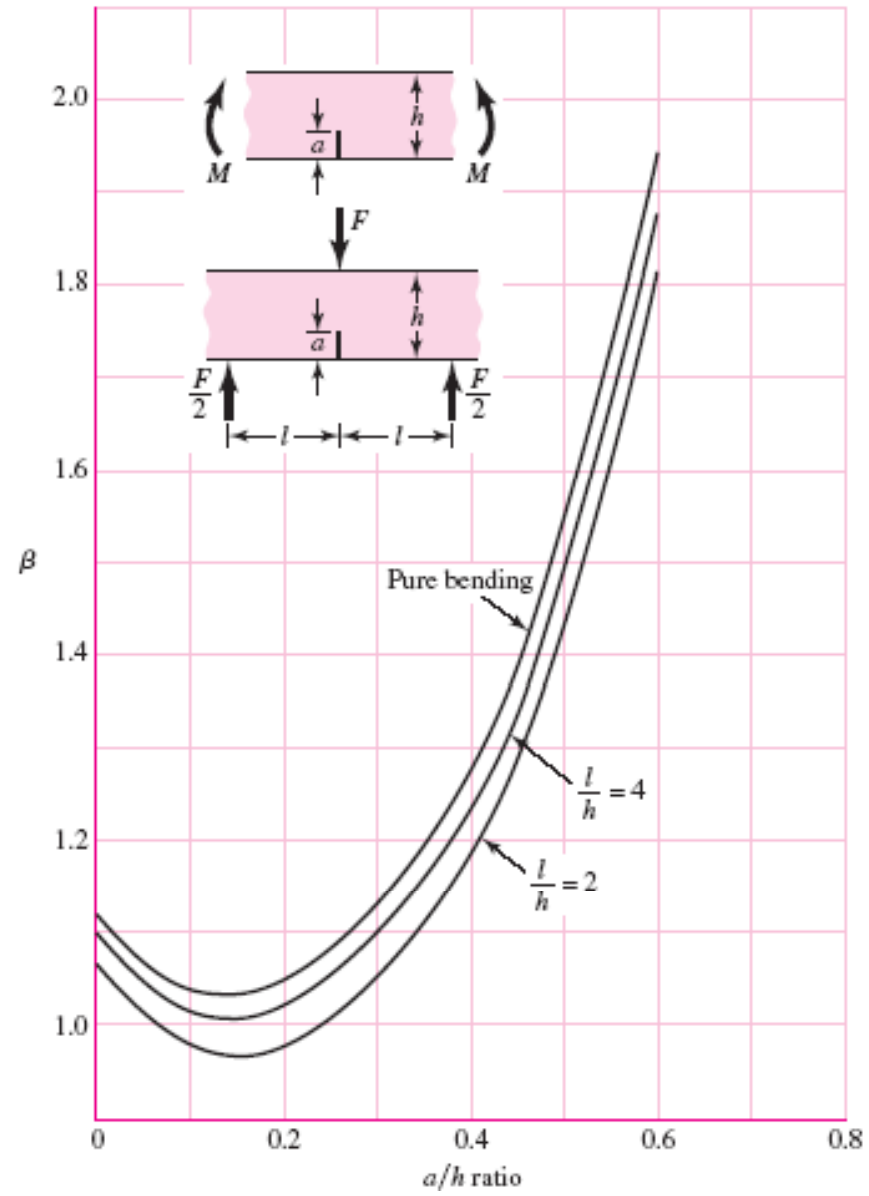
**Figure 5-26**

Plate loaded in longitudinal tension with a crack at the edge; for the solid curve there are no constraints to bending; the dashed curve was obtained with bending constraints added.



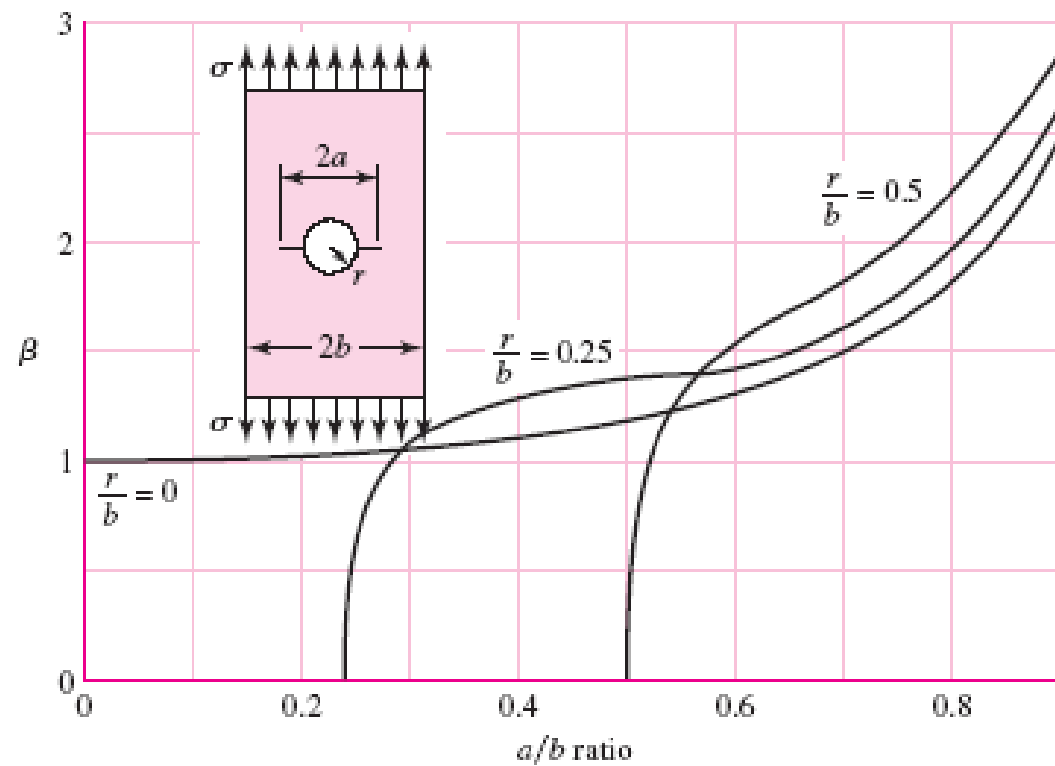
**Figure 5-27**

Beams of rectangular cross section having an edge crack.



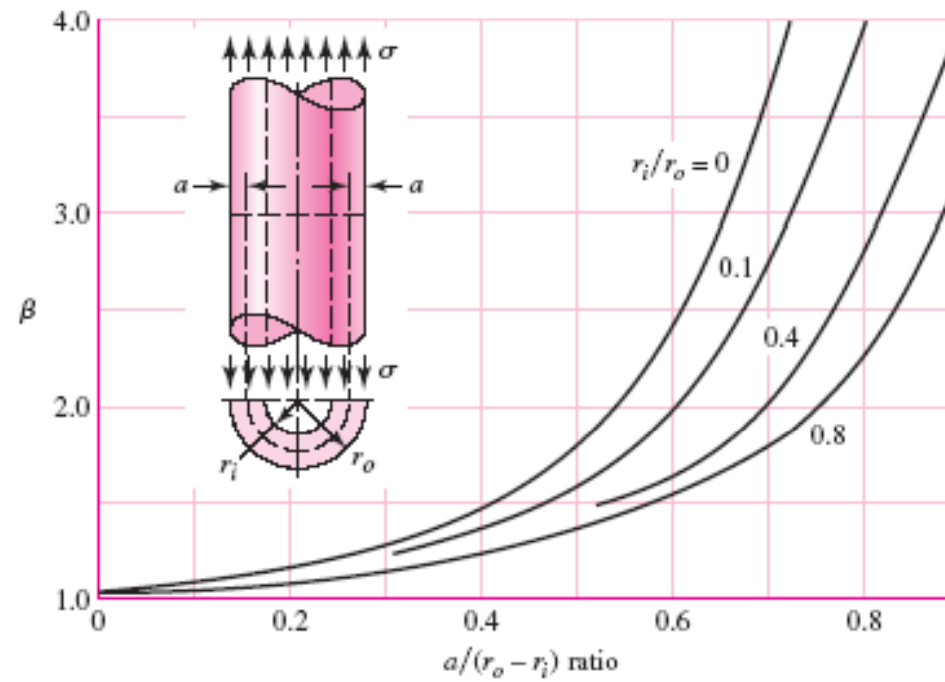
**Figure 5-28**

Plate in tension containing a circular hole with two cracks.



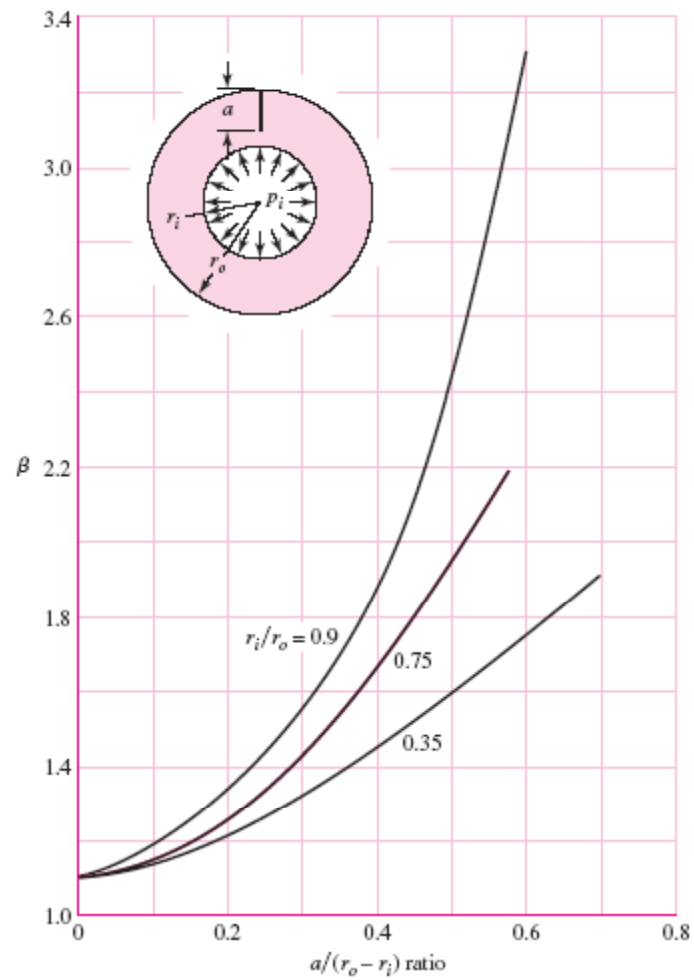
**Figure 5-29**

A cylinder loading in axial tension having a radial crack of depth  $a$  extending completely around the circumference of the cylinder.



**Figure 5-30**

Cylinder subjected to internal pressure  $p_i$  having a radial crack in the longitudinal direction of depth  $a$ . Use Eq. (4-51) for the tangential stress at  $r = r_0$ .



One of the first problems facing the designer is that of deciding whether the conditions exist, or not, for a brittle fracture. Low-temperature operation, that is, operation below room temperature, is a key indicator that brittle fracture is a possible failure mode. Tables of transition temperatures for various materials have not been published, possibly because of the wide variation in values, even for a single material. Thus, in many situations, laboratory testing may give the only clue to the possibility of a brittle fracture. Another key indicator of the possibility of fracture is the ratio of the yield strength to the ultimate strength. A high ratio of  $S_y/S_u$  indicates there is only a small ability to absorb energy in the plastic region and hence there is a likelihood of brittle fracture.

The strength-to-stress ratio  $K_{Ic}/K_I$  can be used as a factor of safety as

$$n = \frac{K_{Ic}}{K_I} \quad (5-38)$$

**EXAMPLE 5-6**

A steel ship deck plate is 30 mm thick and 12 m wide. It is loaded with a nominal uniaxial tensile stress of 50 MPa. It is operated below its ductile-to-brittle transition temperature with  $K_{Ic}$  equal to 28.3 MPa. If a 65-mm-long central transverse crack is present, estimate the tensile stress at which catastrophic failure will occur. Compare this stress with the yield strength of 240 MPa for this steel.

**Solution**

For Fig. 5-25, with  $d = b$ ,  $2a = 65$  mm and  $2b = 12$  m, so that  $d/b = 1$  and  $a/d = 65/12(10^3) = 0.00542$ . Since  $a/d$  is so small,  $\beta = 1$ , so that

$$K_I = \sigma \sqrt{\pi a} = 50 \sqrt{\pi (32.5 \times 10^{-3})} = 16.0 \text{ MPa } \sqrt{\text{m}}$$

From Eq. (5-38),

$$n = \frac{K_{Ic}}{K_I} = \frac{28.3}{16.0} = 1.77$$

The stress at which catastrophic failure occurs is

**Answer**

$$\sigma_c = \frac{K_{Ic}}{K_I} \sigma = \frac{28.3}{16.0} (50) = 88.4 \text{ MPa}$$

The yield strength is 240 MPa, and catastrophic failure occurs at  $88.4/240 = 0.37$ , or at 37 percent of yield. The factor of safety in this circumstance is  $K_{Ic}/K_I = 28.3/16 = 1.77$  and *not*  $240/50 = 4.8$ .



**EXAMPLE 5-7**

A plate of width 1.4 m and length 2.8 m is required to support a tensile force in the 2.8-m direction of 4.0 MN. Inspection procedures will detect only through-thickness edge cracks larger than 2.7 mm. The two Ti-6AL-4V alloys in Table 5-1 are being considered for this application, for which the safety factor must be 1.3 and minimum weight is important. Which alloy should be used?

**Solution**

(a) We elect first to estimate the thickness required to resist yielding. Since  $\sigma = P/wt$ , we have  $t = P/w\sigma$ . For the weaker alloy, we have, from Table 5-1,  $S_y = 910$  MPa. Thus,

$$\sigma_{\text{all}} = \frac{S_y}{n} = \frac{910}{1.3} = 700 \text{ MPa}$$

Thus

$$t = \frac{P}{w\sigma_{\text{all}}} = \frac{4.0(10)^3}{1.4(700)} = 4.08 \text{ mm or greater}$$

For the stronger alloy, we have, from Table 5-1,

$$\sigma_{\text{all}} = \frac{1035}{1.3} = 796 \text{ MPa}$$

and so the thickness is

**Answer**

$$t = \frac{P}{w\sigma_{\text{all}}} = \frac{4.0(10)^3}{1.4(796)} = 3.59 \text{ mm or greater}$$

(b) Now let us find the thickness required to prevent crack growth. Using Fig. 5–26, we have

$$\frac{h}{b} = \frac{2.8/2}{1.4} = 1 \quad \frac{a}{b} = \frac{2.7}{1.4(10^3)} = 0.001\,93$$

Corresponding to these ratios we find from Fig. 5–26 that  $\beta \doteq 1.1$ , and  $K_I = 1.1\sigma\sqrt{\pi a}$ .

$$n = \frac{K_{Ic}}{K_I} = \frac{115\sqrt{10^3}}{1.1\sigma\sqrt{\pi a}}, \quad \sigma = \frac{K_{Ic}}{1.1n\sqrt{\pi a}}$$

From Table 5–1,  $K_{Ic} = 115 \text{ MPa } \sqrt{\text{m}}$  for the weaker of the two alloys. Solving for  $\sigma$  with  $n = 1$  gives the fracture stress

$$\sigma = \frac{115}{1.1\sqrt{\pi(2.7 \times 10^{-3})}} = 1135 \text{ MPa}$$

which is greater than the yield strength of 910 MPa, and so yield strength is the basis for the geometry decision. For the stronger alloy  $S_y = 1035 \text{ MPa}$ , with  $n = 1$  the fracture stress is

$$\sigma = \frac{K_{Ic}}{nK_I} = \frac{55}{1(1.1)\sqrt{\pi(2.7 \times 10^{-3})}} = 542.9 \text{ MPa}$$

which is less than the yield strength of 1035 MPa. The thickness  $t$  is

$$t = \frac{P}{w\sigma_{\text{all}}} = \frac{4.0(10^3)}{1.4(542.9/1.3)} = 6.84 \text{ mm or greater}$$

This example shows that the fracture toughness  $K_{Ic}$  limits the geometry when the stronger alloy is used, and so a thickness of 6.84 mm or larger is required. When the weaker alloy is used the geometry is limited by the yield strength, giving a thickness of only 4.08 mm or greater. Thus the weaker alloy leads to a thinner and lighter weight choice since the failure modes differ.

Determining KIC Experimentally